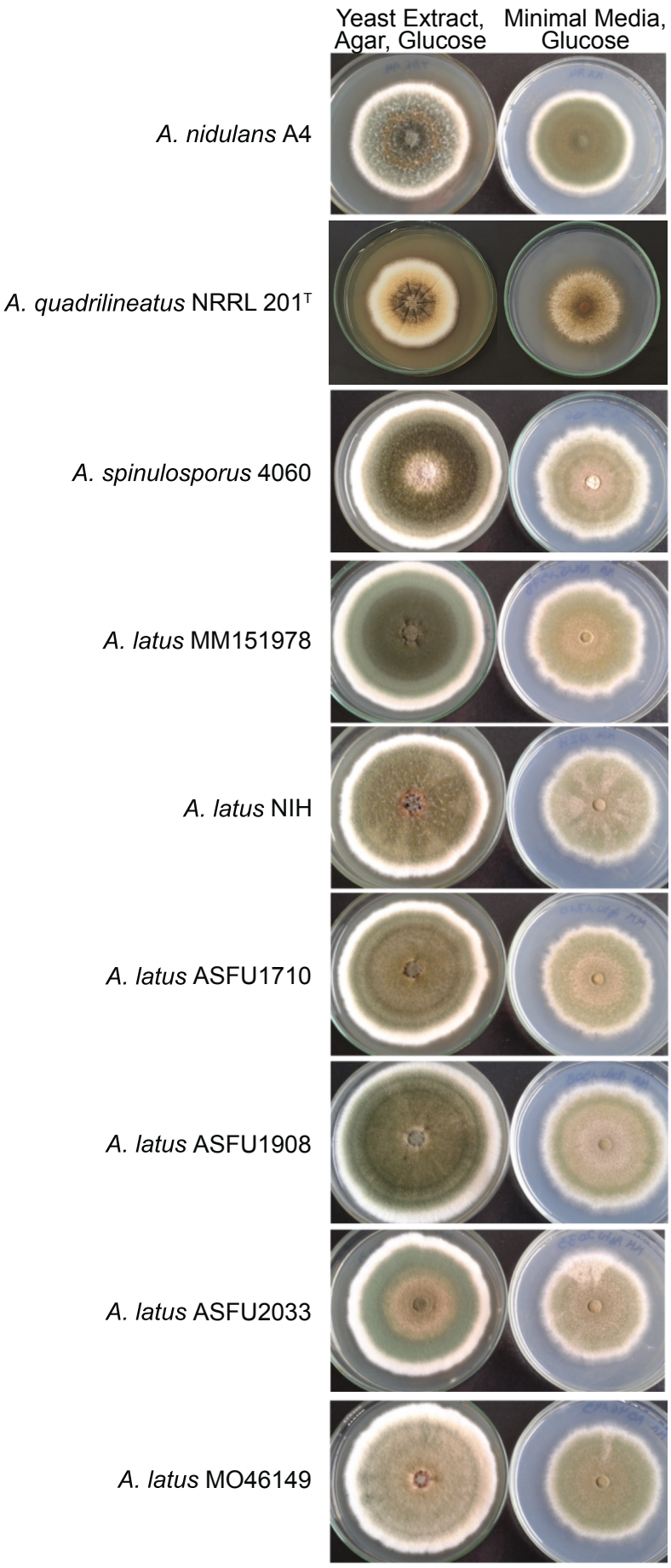
Yeast Extract, Agar, Glucose
Minimal Media, Glucose
A. nidulans A4
A. quadrilineatus NRRL 201T
A. spinulosporus 4060
A. latus MM151978
A. latus NIH
A. latus ASFU1710
A. latus ASFU1908
A. latus ASFU2033
A. latus MO46149

Figure S1. The growth and appearance of the 7 clinical isolates is similar to those of *Aspergillus nidulans*. Related to Figure 1, Table 1 and STAR Methods. Clinical isolates were originally identified as *A. nidulans*. Growth in yeast extract, agar, and glucose (YAG) media and in minimal media supplemented with glucose reveals that the growth and appearance of the clinical isolates appears to be superficially similar to those of the reference A4 strain of *A. nidulans*. We also included *A. quadrilineatus* NRRL 201^{T} for comparative purposes.

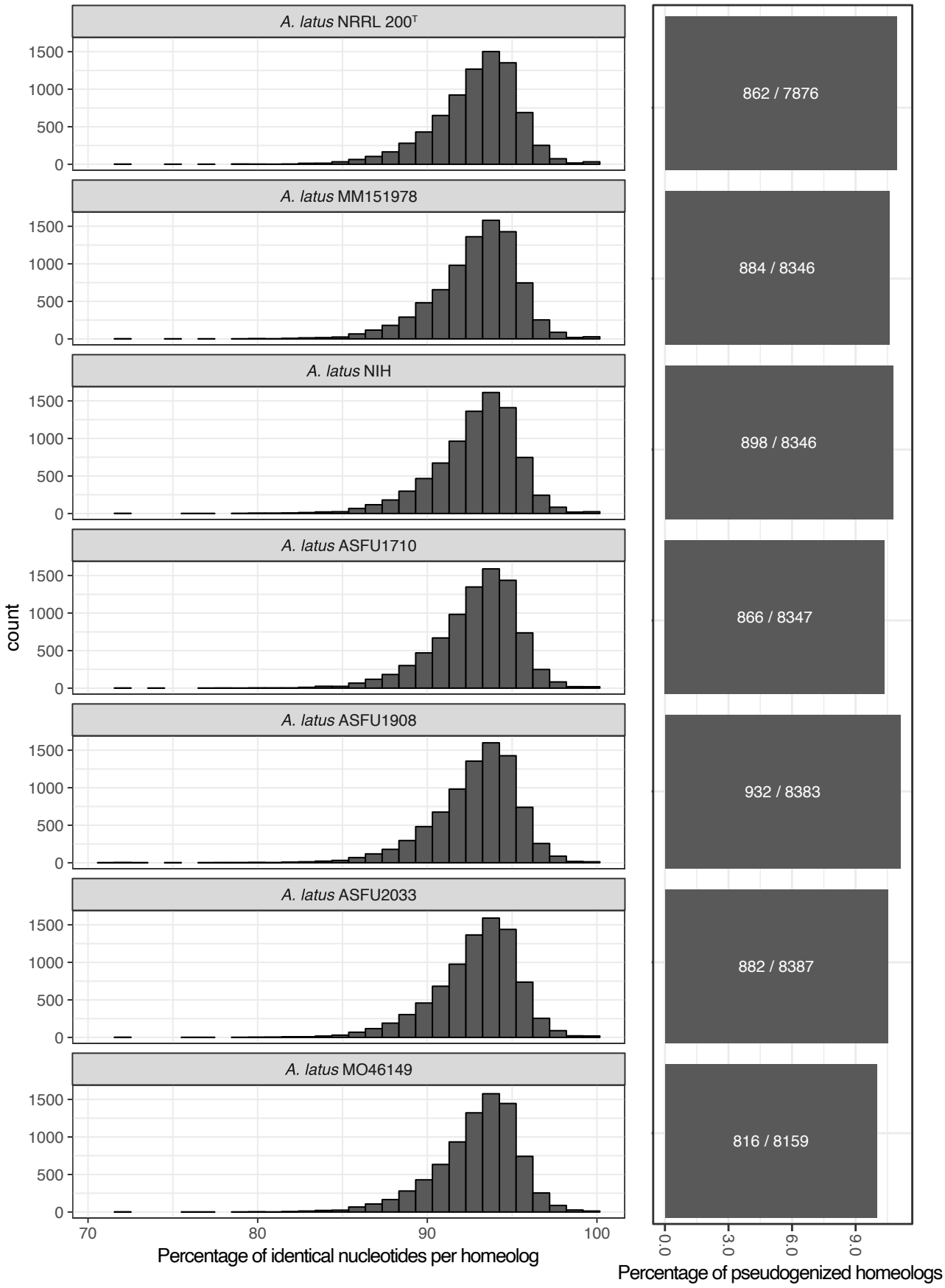
A. latus NRRL 200T
A. latus MM151978
A. latus NIH
A. latus ASFU1710
A. latus ASFU1908
A. latus ASFU2033
A. latus MO46149
count
0
500
1000
1500
70
80
90
100
Percentage of identical nucleotides per homeolog
862 / 7876
884 / 8346
898 / 8346
866 / 8347
932 / 8383
882 / 8387
816 / 8159
0.0
3.0
6.0
9.0
Percentage of pseudogenized homeologs

Figure S2. The parental genomes of *A. latus* hybrid isolates exhibit considerable sequence divergence and have undergone little pseudogenization. Related to Figure 2. (Left) Homeologous gene pairs in *A. latus* genomes were identified using a reciprocal best blast hit approach. Sequence similarity of each gene pair was measured by the percentage of identical nucleotides per homeolog. Across the 7 *A. latus* hybrids, homeolog nucleotide sequence similarity is 92.85 ± 0.03% suggesting the parental genomes are ~7.15% diverged from one another. This level of divergence is on par with the sequence divergence observed between humans and lemurs (*Homo sapiens* vs. *Microcebus murinus* divergence measured using the same reciprocal best blast hit approach is 8.36%). (Right) The average percentage of pseudogenized homeologs in *A. latus* hybrid isolates is 11.67 ± 0.004%. The percentage of pseudogenized homeologs in each hybrid isolate was calculated by comparing gene lengths between homeologs. One gene in a homeolog pair was considered pseudogenized if their length was shorter (upper threshold of 80%) than the other gene in the homeolog pair.

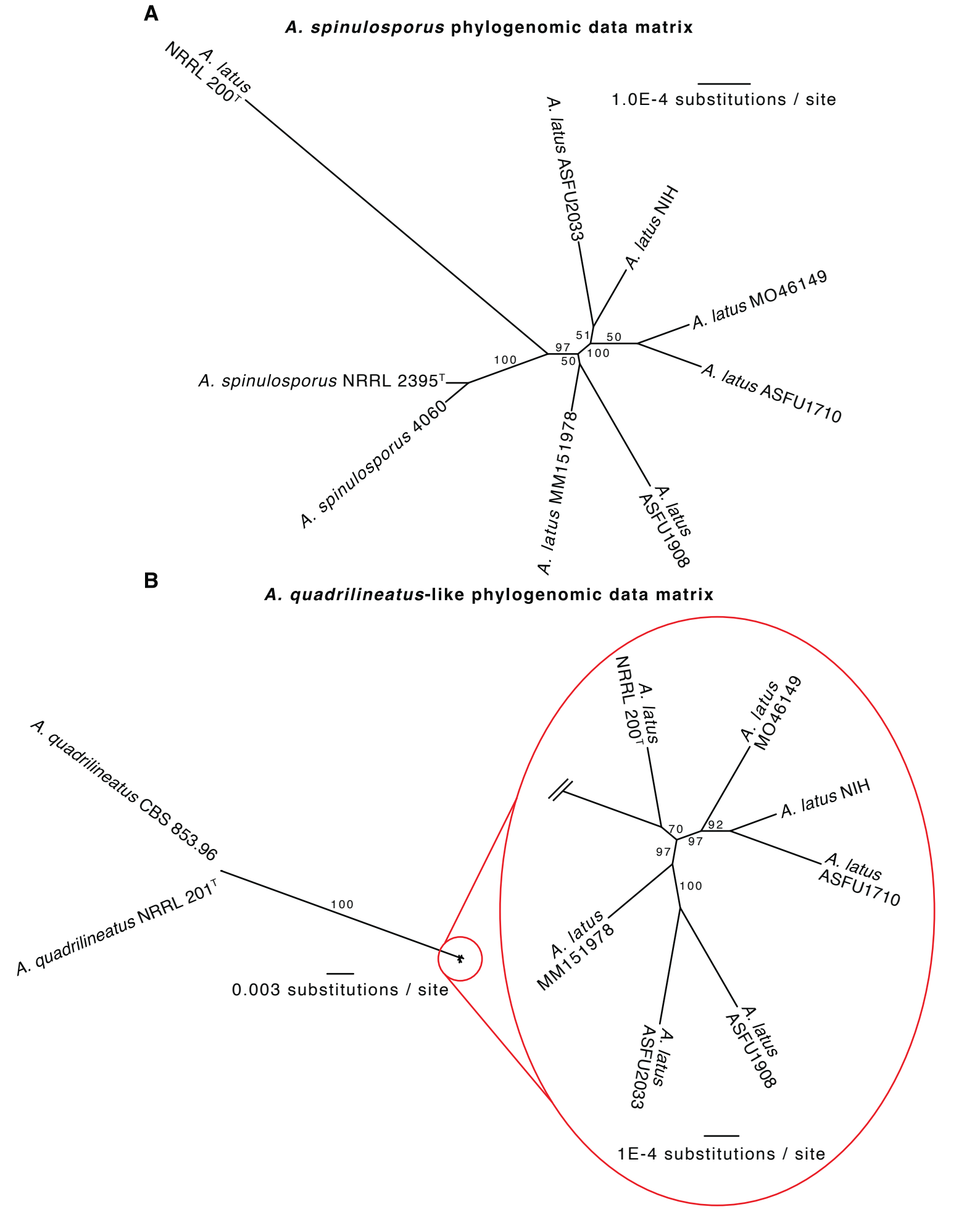
A
A. spinulosporus phylogenomic data matrix
A. latus NRRL 200T
1.0E-4 substitutions / site
A. latus ASFU2033
A. latus NIH
A. latus MO46149
A. latus ASFU1710
A. spinulosporus NRRL 2395T
A. spinulosporus 4060
A. latus MM151978
A. latus ASFU1908
51
50
97
100
50
100
B
A. quadrilineatus-like phylogenomic data matrix
A. quadrilineatus CBS 853.96
A. quadrilineatus NRRL 201T
100
0.003 substitutions / site
A. latus NRRL 200T
A. latus MO46149
A. latus NIH
A. latus ASFU1710
A. latus MM151978
A. latus ASFU2033
A. latus ASFU1908
70
92
97
97
100
1E-4 substitutions / site

Figure S3. The evolutionary histories of the two parental genomes of *A. latus* hybrid isolates are consistent with each other and support genome-wide instability in the *A. latus* type strain NRRL 200. Related to Figure 2 and Data S1. Evolutionary histories were reconstructed from data matrices of single-copy orthologous genes from either the (A) *A. latus* parental genome from *A. spinulosporus* and true *A. spinulosporus* strains or (B) *A. latus* parental genome from *A. quadrilineatus*-like species and true *A. quadrilineatus* strains. While the two topologies differ, application of approximately unbiased topology constraint tests showed that the two topologies were not statistically different from each other (p-value = 0.50 for both tests). These results are consistent with the hypothesis that the two parental genomes of *A. latus* share the same evolutionary history. The long branch of *A. latus* NRRL 200 inferred using the *A. spinulosporus* phylogenomic data matrix likely reflects potential genomic instability. Branch lengths represent substitutions per site. Bipartition support was assessed using 5,000 ultrafast bootstrap approximations.

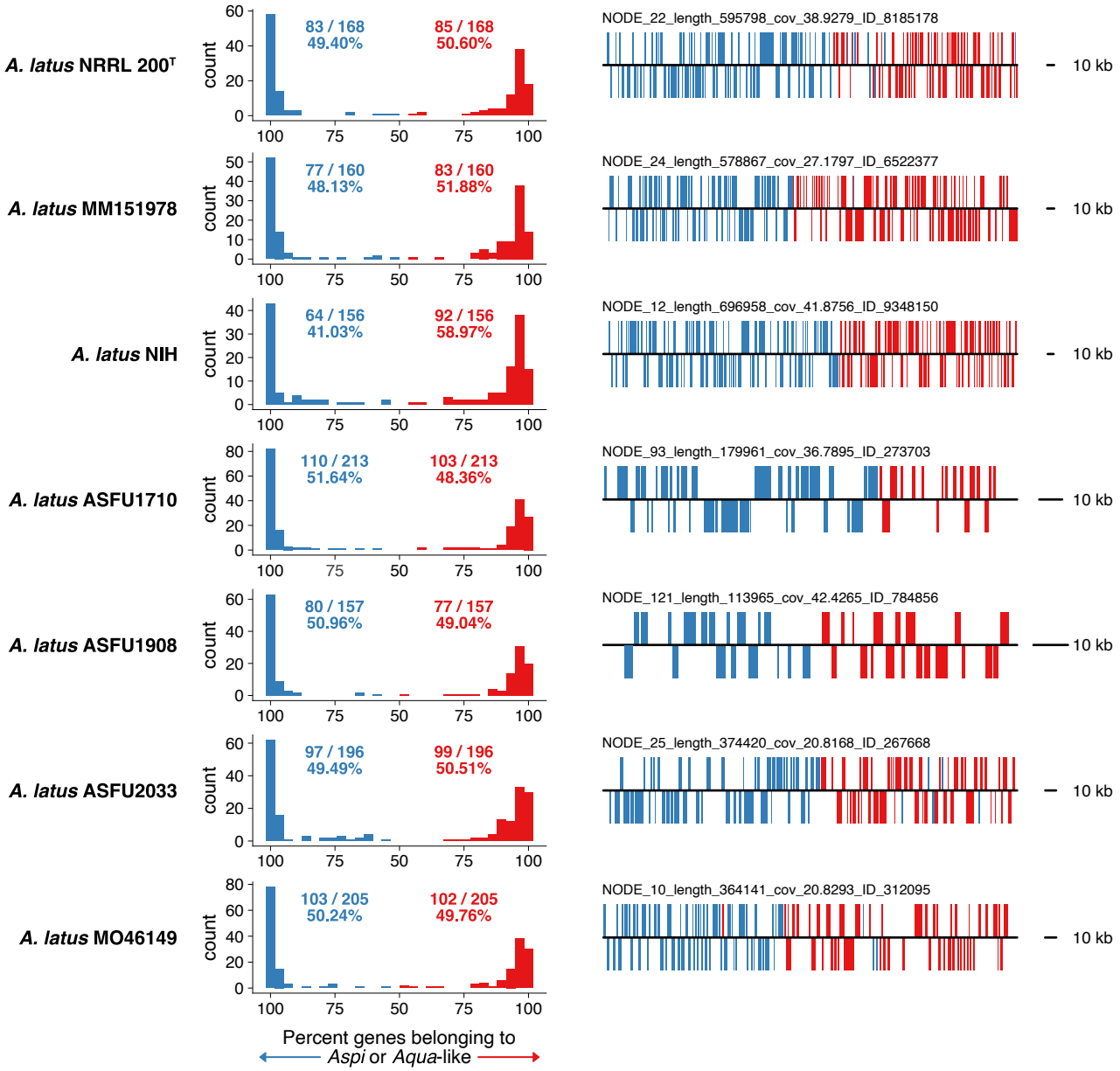
A. latus NRRL 200T
A. latus MM151978
A. latus NIH
A. latus ASFU1710
A. latus ASFU1908
A. latus ASFU2033
A. latus MO46149
count
83 / 168
49.40%
85 / 168
50.60%
77 / 160
48.13%
83 / 160
51.88%
64 / 156
41.03%
92 / 156
58.97%
110 / 213
51.64%
103 / 213
48.36%
80 / 157
50.96%
77 / 157
49.04%
97 / 196
49.49%
99 / 196
50.51%
103 / 205
50.24%
102 / 205
49.76%
Percent genes belonging to
Aspi or Aqua-like
NODE_22_length_595798_cov_38.9279_ID_8185178
NODE_24_length_578867_cov_27.1797_ID_6522377
NODE_12_length_696958_cov_41.8756_ID_9348150
NODE_93_length_179961_cov_36.7895_ID_273703
NODE_121_length_113965_cov_42.4265_ID_784856
NODE_25_length_374420_cov_20.8168_ID_267668
NODE_10_length_364141_cov_20.8293_ID_312095
10 kb

Figure S4. Lack or very low levels of recombination between the parental genomes. Related to Figure 2 and Data S1. For each genomic contig of each *A. latus* hybrid, we examined the percentage of genes that came from one or the other parent (left column); exemplary contigs (one for each hybrid) that are putatively the result of a recombinant event are shown on the right column. Contig of origin analysis was conducted by examining the percentage of genes on long contigs (≥ 100 kb in length) from either the *A. spinulosporus* parent (*Aspi*; blue) or the *A. quadrilineatus*-like parent (*Aqua*-like; red). Contigs that are predominantly of *A. spinulosporus* are shown on the left side of the distributions and contigs that are predominantly *A. quadrilineatus*-like on the right side. We considered contigs that contained substantial percentages of genes from both parents to be putatively recombinant. For example, 2.67 ± 0.71% of *A. latus* hybrid contigs contain between 35% and 65% of genes from both parents. Exemplary contigs with evidence of recombination contain genes from the *A. spinulosporus* parent on one side and genes from the *A. quadrilineatus*-like parent on the other. Contigs are represented by black lines a key for contig length is shown to the right. For each contig, the entirety of the contig is depicted and the contig identifier is also provided. Genes on different strands of DNA are depicted either above or below the black line.

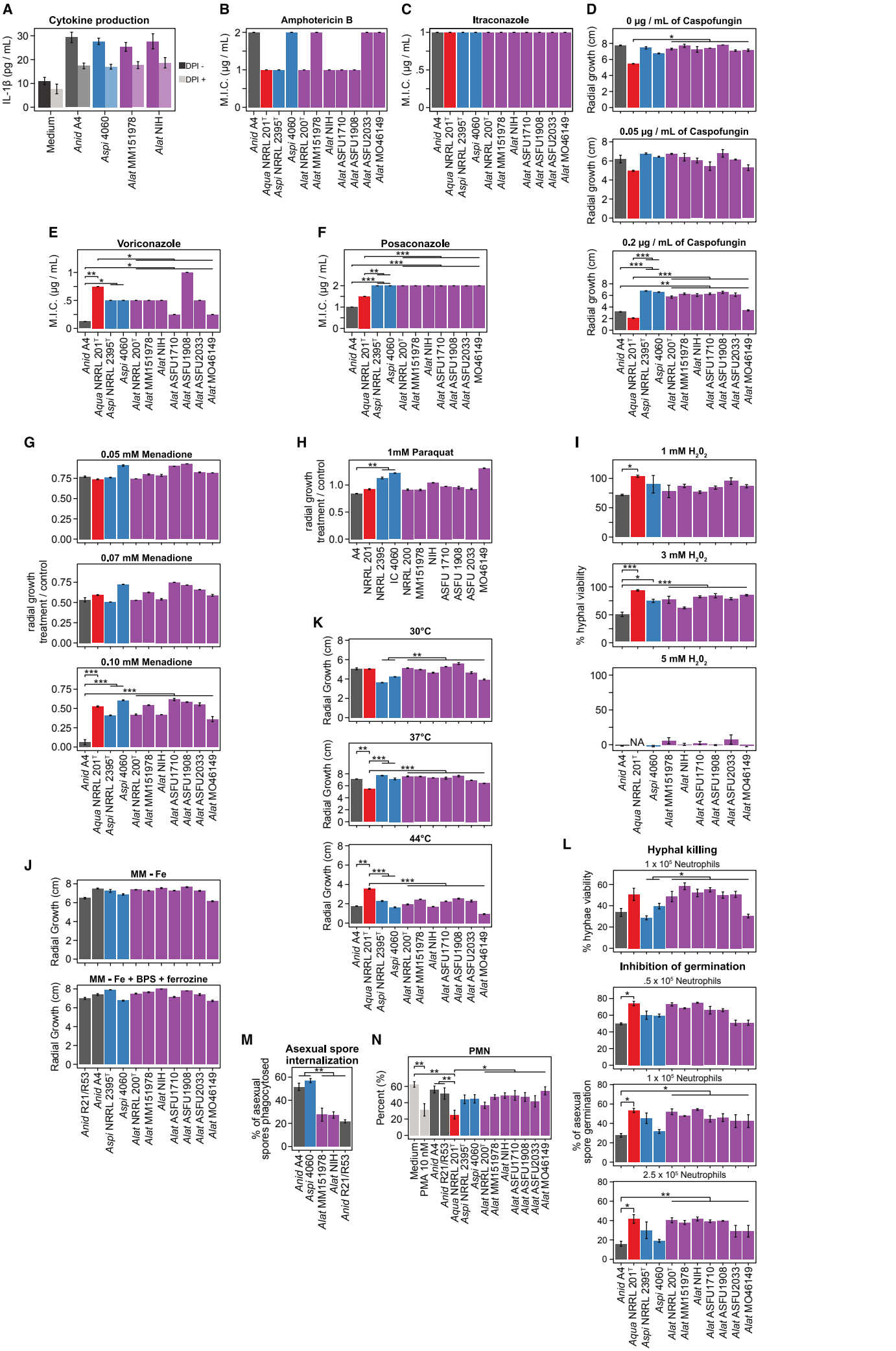
A
Cytokine production
IL-1β (pg / mL)
DPI -
DPI +
Medium
Anid A4
Aspi 4060
Alat MM151978
Alat NIH
B
Amphotericin B
M.I.C. (µg / mL)
C
Itraconazole
D
0 µg / mL of Caspofungin
0.05 µg / mL of Caspofungin
0.2 µg / mL of Caspofungin
Radial growth (cm)
E
Voriconazole
F
Posaconazole
G
0.05 mM Menadione
0.07 mM Menadione
0.10 mM Menadione
radial growth treatment / control
H
1mM Paraquat
I
1 mM H2O2
3 mM H2O2
5 mM H2O2
% hyphal viability
J
MM - Fe
MM - Fe + BPS + ferrozine
K
30°C
37°C
44°C
L
Hyphal killing
1 x 10⁵ Neutrophils
% hyphae viability
Inhibition of germination
.5 x 10⁵ Neutrophils
2.5 x 10⁵ Neutrophils
% of asexual spore germination
M
Asexual spore internalization
% of asexual spores phagocytosed
N
PMN
Percent (%)
Anid A4
Aqua NRRL 201T
Aspi NRRL 2395T
Aspi 4060
Alat NRRL 200T
Alat MM151978
Alat NIH
Alat ASFU1710
Alat ASFU1908
Alat ASFU2033
Alat MO46149
Anid R21/R53

Figure S5. Phenotypic characterization of diverse infection-relevant traits among *A. nidulans, A. spinulosporus*, *A. quadrilineatus*, and *A. latus* hybrid isolate and strains. **Related to Figure 3.** (A) Examination of cytokine production (i.e., macrophage response) to co-culture with no *Aspergillus* species, *A. nidulans* A4, *A. spinulosporus* strain 4060, and *A. latus* strain MM151978 and NIH revealed no significant difference in cytokine production with and without diphenylene iodonium (DPI). (B and C) Examination of minimum inhibitory concentration (MIC) in amphotericin B and itraconazole revealed no statistically significant difference between the various species. (D) Examination of susceptibility to caspofungin revealed statistically significant differences in some concentrations, which are shown and discussed in Figure 3. (E) Statistically significant differences in MIC of voriconazole among the various species ($\chi^2 = 14.44$, df = 3, $p = 0.002$; Kruskal-Wallis rank sum test). (F) Examination of the MIC for posaconazole reveals significant differences among the various species ($\chi^2 = 32$, df = 3, $p < 0.001$; Kruskal-Wallis rank sum test). (G) Examination of radial growth in the presence of the oxidative stressor menadione revealed significant differences among the three species at different concentrations of menadione ($F(6) = 7.01$, $p < 0.001$; Multi-factor ANOVA). (H) Statistically significant differences were observed in the growth of paraquat (see also Figure 3). (I) Significant differences in radial growth among *A. nidulans, A. spinulosporus,* and *A. latus* hybrids in the presence of H_20_2 ($F(6) = 3.00$, $p = 0.009$; Multi-factor ANOVA). (J) No statistically significant differences were observed in iron starvation assays. (K) Significant differences were observed in the growth of the various species at different temperatures ($F(6) = 15.65$, $p < 0.001$; Multi-factor ANOVA). (M) Significant differences were observed in asexual spore internalization by macrophages between diploid (*A. latus* MM151978, *A. latus* NIH, and *A. nidulans* R21/R53) and haploid genomes (*A. nidulans* A4 and *A. spinulosporus* 4060) ($p < 0.001$;

Wilcoxon Rank Sum test). (N) Statistically significant differences were observed in NETosis. Shown here is the percentage of Human polymorphonuclear cells surviving co-culture with the fungus (see also Figure 3). (L) Statistically significant differences were observed in hyphal killing by macrophages (see also Figure 3). Additionally, significant differences were observed in the inhibition of fungal germination by macrophages among the various species ($F(3) = 20.61$, $p < 0.001$; Multi-factor ANOVA). For multi-factor ANOVAs, all pairwise comparisons were made using a Tukey Honest Significant differences test; for Kruskal-Wallis rank sum tests, pairwise comparisons were made using a Dunn's test with multi-test correction using the Benjamini-Hochberg procedure. * represents p-values less than 0.05 but greater than 0.01; ** represents p-values less than 0.01 but greater than 0.001; *** represents p-values less than 0.001.

Genome	Genome Size	N50*	Number of genes
A. quadrilineatus NRRL 201^{T}	32,509,921	293,960	10,234
A. quadrilineatus CBS 853.96	34,797,351	229,104	11,183
4060	31,665,638	425,600	9,499
A. latus NRRL 200^{T}	62,482,878	383,812	18,918
MM151978	64,066,396	422,061	19,490
NIH	66,248,764	400,658	19,760
ASFU1710	78,387,730	125,661	24,333
ASFU1908	74,406,717	73,356	24,753
ASFU2033	69,995,940	181,936	21,380
MO46149	68,059,968	124,885	20,617

Table S1. Genome assembly size, N50, and number of predicted genes. Related to Figure 1.

***N50: the contig size where 50% of the genome assembly is contained in contigs equal or larger than its size.**

Genome	Total	Type 1 PKS	NRPS	Type 3 PKS	Terpene	Indole	Multiple	Other
A. nidulans A4	53	18	9	0	6	3	7	10
A. quadrilineatus NRRL 201^T	69	26	10	0	10	4	7	12
A. spinulosporus NRRL2395	53	19	8	0	9	3	7	7
4060	54	20	8	0	9	3	7	7
A. latus NRRL 200^T	111	41	16	0	14	6	16	18
MM151978	115	43	16	0	15	7	17	17
NIH	114	42	18	0	15	6	16	17
ASFU1710	123	47	17	0	15	7	16	21
ASFU1908	131	54	20	1	19	8	10	19
ASFU2033	120	48	17	0	17	8	13	17
MO46149	116	46	18	0	17	6	10	19

Table S2. Number of predicted secondary metabolic gene clusters per genome. Related to Figure 1.

Genome Assembly or Raw Reads	**BioProject**	**BioSample**	**Accession**	**Genus**	**Species**	**Strain**
Genome Assembly	PRJNA542678	SAMN11621154	VCRF00000000	*Aspergillus*	*spinulosporus*	4060
Genome Assembly	PRJNA542678	SAMN11615383	VCRG00000000	*Aspergillus*	*latus*	MO46149
Genome Assembly	PRJNA542678	SAMN11615382	VCRH00000000	*Aspergillus*	*latus*	ASFU2033
Genome Assembly	PRJNA542678	SAMN11615381	VCRI00000000	*Aspergillus*	*latus*	ASFU1908
Genome Assembly	PRJNA542678	SAMN11615380	VCRJ00000000	*Aspergillus*	*latus*	ASFU1710

Genome Assembly	PRJNA542678	SAMN11615379	VCRK00000000	*Aspergillus*	*latus*	NIH
Genome Assembly	PRJNA542678	SAMN11615378	VCRL00000000	*Aspergillus*	*latus*	MM151978
Genome Assembly	PRJNA542141	SAMN11612423	VCRM00000000	*Aspergillus*	*latus*	NRRL 200^{T}
Genome Assembly	PRJNA623402	See BioProject	See BioProject	*Aspergillus*	*quadrilineatus*	NRRL 201^{T}
Raw Reads	PRJNA542395	N/A	N/A	*Aspergillus*	*spinulosporus*	4060
Raw Reads	PRJNA542181	N/A	N/A	*Aspergillus*	*latus*	MO46149
Raw Reads	PRJNA542181	N/A	N/A	*Aspergillus*	*latus*	ASFU2033
Raw Reads	PRJNA542181	N/A	N/A	*Aspergillus*	*latus*	ASFU1908
Raw Reads	PRJNA542181	N/A	N/A	*Aspergillus*	*latus*	ASFU1710

Raw Reads	PRJNA542181	N/A	N/A	*Aspergillus*	*latus*	NIH
Raw Reads	PRJNA542181	N/A	N/A	*Aspergillus*	*latus*	MM151978
Raw Reads	PRJNA542141	N/A	N/A	*Aspergillus*	*latus*	NRRL 200^{T}
Raw Reads	PRJNA623402	See BioProject	See BioProject	*Aspergillus*	*quadriliena tus*	NRRL 201^{T}

Table S3. NCBI accession information for each sequenced genome.